PHYSICAL REVIEW D **91,** 074003 (2015)

Near-threshold $\bar{p}p$ invariant mass spectrum measured in J/ψ and ψ' decays

Xian-Wei Kang,[1,*] Johann Haidenbauer,[1,†] and Ulf-G. Meißner[1,2,‡]

[1]*Institute for Advanced Simulation, Jülich Center for Hadron Physics, and Institut für Kernphysik, Forschungszentrum Jülich, D-52425 Jülich, Germany*

[2]*Helmholtz-Institut für Strahlen- und Kernphysik and Bethe Center for Theoretical Physics, Universität Bonn, D-53115 Bonn, Germany*

(Received 9 February 2015; published 2 April 2015)

A systematic analysis of the near-threshold enhancement in the $\bar{p}p$ invariant mass spectrum seen in the decay reactions $J/\psi \to x\bar{p}p$ and $\psi(3686) \to x\bar{p}p$ $(x = \gamma, \omega, \rho, \pi, \eta)$ is presented. The enhancement is assumed to be due to the $\bar{N}N$ final-state interaction (FSI) and the pertinent FSI effects are evaluated in an approach that is based on the distorted-wave Born approximation. For the $\bar{N}N$ interaction a recent potential derived within chiral effective field theory and fitted to results of a partial-wave analysis of $\bar{p}p$ scattering data is considered and, in addition, an older phenomenological model constructed by the Jülich group. It is shown that the near-threshold spectrum observed in various decay reactions can be reproduced simultaneously and consistently by our treatment of the $\bar{p}p$ FSI. It turns out that the interaction in the isospin-1 $^1S_0$ channel required for the description of the $J/\psi \to \gamma\bar{p}p$ decay predicts a $\bar{N}N$ bound state.

DOI: 10.1103/PhysRevD.91.074003 PACS numbers: 12.39.Fe, 13.25.Gv, 13.75.Cs, 25.43.+t

I. INTRODUCTION

The origin of the enhancement in the antiproton-proton ($\bar{p}p$) mass spectrum at low invariant masses observed in heavy meson decays like $J/\psi \to \gamma\bar{p}p$, $B \to K\bar{p}p$ and $\bar{B} \to D\bar{p}p$, but also in the reaction $e^+e^- \leftrightarrow \bar{p}p$, is an interesting and still controversially discussed issue. In particular, the spectacular near-threshold enhancement in the $\bar{p}p$ invariant mass spectrum for the reaction $J/\psi \to \gamma\bar{p}p$, first observed in a high-statistics and high-mass-resolution experiment by the BES Collaboration [1], has led to numerous publications with speculations about the discovery of a new resonance [1] or of a $\bar{p}p$ bound state (baryonium) [2–4], and was even associated with exotic glueball states [5–7]. However, in the above processes the hadronic final-state interaction (FSI) in the $\bar{p}p$ system should play a role too. Indeed, the group in Jülich-Bonn [8,9] but also others [10–17] demonstrated that the near-threshold enhancement in the $\bar{p}p$ invariant mass spectrum of the reaction $J/\psi \to \gamma\bar{p}p$ could be simply due to the FSI between the outgoing proton and antiproton. Specifically, the calculation [8,9] based on the realistic Jülich antinucleon–nucleon ($\bar{N}N$) model [18–20], the one by the Paris group [15], utilizing the Paris $\bar{N}N$ model [21], and that of Entem and Fernández [14], using a $\bar{N}N$ interaction derived from a constituent quark model [22], explicitly confirmed the significance of FSI effects estimated in the initial studies [10–12] within the effective range approximation.

In the present work we perform a systematic analysis of the near threshold enhancements in the reactions $J/\psi \to x\bar{p}p$ and $\psi'(3686) \to x\bar{p}p$ $(x = \gamma, \omega, \rho, \pi, \eta)$ with emphasis on the role played by the $\bar{p}p$ interaction. The aim is to achieve a simultaneous and consistent description of all $\bar{p}p$ invariant mass spectra measured in the various reactions. FSI effects for different decay channels cannot be expected to be quantitatively the same. In particular, with regard to $\bar{p}p$, the two baryons have to be in different states if the quantum numbers of the third particle in the decay channel differ, in accordance with the general conservation laws. Furthermore, it is possible that dynamical selection rules, reflecting the details of the reaction mechanism, could suppress the decay into $\bar{p}p$ S-waves for some decays near threshold. Thus, in different decay modes the final $\bar{p}p$ system can and must be in different partial waves and, accordingly the FSI effects will differ too.

As mentioned, initial studies of FSI effects in the decay $J/\psi \to \gamma\bar{p}p$ were done in the rather simplistic effective range approximation. Later investigations, like the ones performed by us [8,9], employed directly scattering amplitudes from realistic $\bar{N}N$ potential models. Still also here the treatment of the FSI is done within the so-called Migdal-Watson approach [23,24] where the elementary decay (or production) amplitude is simply multiplied with the $\bar{p}p$ T-matrix. It is known that this approach works reasonably well for reactions with a final NN system [25]. In this case the scattering length a is fairly large, for example, $a \approx -24$ fm for a final np system (in the $^1S_0$ state). Measurements of the level shifts in antiprotonic hydrogen atoms suggest that the scattering lengths for $\bar{p}p$ scattering are presumably only in the order of 1 to 2 fm [26]. Moreover, those scattering lengths are complex due to

*x.kang@fz-juelich.de
†j.haidenbauer@fz-juelich.de
‡meissner@hiskp.uni-bonn.de

 © 2015 American Physical Society

the presence of annihilation channels. Therefore, in the present paper we consider an alternative and more refined approach for taking into account the FSI. Specifically, we use the Jost function which is calculated directly from realistic $\bar{N}N$ potentials. FSI effects are then taken into account by multiplying the reaction amplitude with the inverse of this Jost function. This is practically equivalent to a treatment of such decay reactions within a distorted-wave Born approximation. Note that this is different from the popular Jost-function approach based on the effective range approximation [27] which is widely used in investigations of FSI effects.

We present results for the decays $J/\psi \to x\bar{p}p$ with $x = \gamma, \omega, \pi^0, \eta$, which all have been measured. For the last three cases parity, G-parity, and isospin are conserved so that each of those channels allows one to explore the $\bar{p}p$ system in a distinct partial wave. At the same time the analogous reactions $\psi' \to x\bar{p}p$ are studied. In this case there are data for $x = \gamma, \pi^0, \eta$. Clearly, if $\bar{p}p$ FSI effects are responsible for the enhancements seen in specific J/ψ decays, then very similar effects should occur in the corresponding ψ' decays because the selection rules are the same.

As far as the $\bar{N}N$ interaction is concerned we employ again the phenomenological model A(OBE) of the Jülich group [18] used in our earlier works [8,9,28,29]. In addition, and as a novelty, we utilize also a $\bar{N}N$ interaction derived in the framework of chiral effective field theory (EFT) [30]. The latter interaction incorporates results of a recent partial-wave analysis (PWA) of $\bar{p}p$ scattering data [31]. In particular, this EFT potential has been constructed in such a way, that it reproduces the amplitudes determined in the PWA well up to laboratory energies of $T_{lab} \approx$ 200–250 MeV [30], i.e. in the low-energy region where we expect that FSI effects are important.

As pointed out at the beginning, also in decays of the B and Υ mesons to final states with a $\bar{N}N$ pair enhancements at low invariant masses have been observed [32–39]. However, in the majority of those experiments the invariant-mass resolution of the $\bar{N}N$ spectrum is relatively low and often there are only two or three data points in the (relevant) near-threshold region. Therefore, we refrain from looking at those data in detail. Note also, that in case of weak decays like $B \to K\bar{p}p$ or $B \to D\bar{p}p$ parity is not conserved and, as a consequence, there is less restriction on the possible partial waves of the $\bar{N}N$ final state. The situation is different for the reaction $e^+e^- \leftrightarrow \bar{p}p$. As shown by us in recent studies [40,41], employing the same formalism and the same $\bar{N}N$ interactions as in the present work, the FSI mechanism can indeed explain the near-threshold enhancement seen in the data taken by the PS170 [42], the FENICE [43] and the *BABAR* [44] Collaborations.

The paper is structured in the following way: In Sec. II we provide a summary of the formalism that we employ for treating the FSI due to the $\bar{N}N$ interaction. We discuss also the selection rules for the decay channels considered. Results of our calculations are presented in Sec. III. First we analyze hadronic decay channels of J/ψ and ψ' (where isospin is assumed to be conserved) and compare our predictions with measurements of the $\bar{p}p$ invariant mass spectrum for the $\pi^0\bar{p}p$, $\eta\bar{p}p$, and $\omega\bar{p}p$ channels. Subsequently we consider radiative decays. Since it turns out that the $\bar{p}p$ invariant mass spectrum of $J/\psi \to \gamma\bar{p}p$ can no longer be described with the employed and previously established $\bar{N}N$ interactions, once the more realistic treatment of FSI effects is utilized, we perform and present a refit of the chiral EFT $\bar{N}N$ potential that reproduces the $\gamma\bar{p}p$ data and stays also very close to the result of the PWA (and to the original EFT potential [30]) for the relevant ($^1S_0$) partial wave. The paper ends with a summary. Results of the refitted $^1S_0$ $\bar{N}N$ potential are presented in an appendix, and compared with the PWA and the previously published EFT potential [30].

II. TREATMENT OF THE $\bar{N}N$ FINAL STATE INTERACTION

Our study of the processes of J/ψ (or ψ') decaying to $x\bar{p}p$ ($x = \gamma, \omega, \pi, \eta$) is based on the distorted wave Born approximation (DWBA) where the reaction amplitude A is given by

$$A = A^0 + A^0 G^{\bar{N}N} T^{\bar{N}N}. \tag{1}$$

Here A^0 is the elementary (or primary) decay amplitude, $G^{\bar{N}N}$ the free $\bar{N}N$ Green's function, and $T^{\bar{N}N}$ the $\bar{N}N$ scattering amplitude. For a particular (uncoupled) $\bar{N}N$ partial wave with orbital angular momentum L, Eq. (1) reads

$$A_L = A^0_L + \int_0^\infty \frac{dpp^2}{(2\pi)^3} A^0_L \frac{1}{2E_k - 2E_p + i0^+} T_L(p,k;E_k), \tag{2}$$

where T_L denotes the partial-wave projected T-matrix element, and k and E_k are the momentum and energy of the proton (or antiproton) in the center-of-mass system of the $\bar{N}N$ pair. The quantity $T_L(p,k;E_k)$ is obtained from the solution of the Lippmann-Schwinger (LS) equation,

$$T_L(p',k;E_k) = V_L(p',k) + \int_0^\infty \frac{dpp^2}{(2\pi)^3} V_L(p',p) \times \frac{1}{2E_k - 2E_p + i0^+} T_L(p,k;E_k), \tag{3}$$

for a specific $\bar{N}N$ potential V_L. In case of coupled partial waves like the $^3S_1$–$^3D_1$ we solve the corresponding coupled LS equation as given in Eq. (2.20) of Ref. [30], and use then T_{LL} in Eq. (2).

In principle, the elementary production amplitude A_L^0 in Eq. (2) has an energy dependence and it depends also on the $\bar{N}N$ momentum and the photon momentum relative to the $\bar{N}N$ system. However, in the near-threshold region the variation of the production amplitude with regard to those variables should be rather small as compared to the strong momentum dependence induced by the $\bar{N}N$ FSI and, therefore, we neglect it in the following. Then Eq. (2) can be reduced to

$$A_L = \bar{A}_L^0 k^L \left[1 + \int_0^\infty \frac{dp p^2}{(2\pi)^3} \frac{p^L}{k^L} \frac{1}{2E_k - 2E_p + i0^+} T_L(p,k;E_k)\right] = \bar{A}_L^0 k^L \psi_{k,L}^{(-)*}(0). \quad (4)$$

Here, we have separated the factor k^L which ensures the correct threshold behavior for a particular orbital angular momentum so that $\bar{A}_L^0$ is then a constant. The quantity in the bracket in Eq. (4) is the so-called enhancement factor [27]. Introducing a suitably normalized wave function for the $\bar{p}p$ pair in the continuum [27], $\psi_{k,L}^{(-)*}(0)$, this quantity is just the inverse of the Jost function, i.e. $\psi_{k,L}^{(-)*}(0) = f_L^{-1}(-k)$. We want to emphasize that in the present work we calculate the enhancement factor for the considered $\bar{N}N$ interactions explicitly, which amounts to an integral over the pertinent (half-off-shell) T matrix elements, see Eq. (4). This should not be confused with the popular Jost-function approach which relies simply on the effective range approximation. In any case, the latter cannot be easily applied in the $\bar{N}N$ case because now the scattering length as well as the effective range are complex quantities. For a thorough discussion of various aspects of the treatment of FSI effects due to baryon-baryon interactions, see Refs. [45–47].

The differential decay rate for the processes $X \to x\bar{p}p$ ($X = J/\psi, \psi'$) can be written in the form [8,48]

$$\frac{d\Gamma}{dM} = \frac{\lambda^{1/2}(m_X^2, M^2, m_x^2)\sqrt{M^2 - 4m_p^2}}{2^6\pi^3 m_X^2} |A|^2, \quad (5)$$

after integrating over the angles. Here the Källén function λ is defined as $\lambda(x,y,z) = ((x-y-z)^2 - 4yz)/(4x)$, $M \equiv M(\bar{p}p)$ is the invariant mass of the $\bar{p}p$ system, m_X, m_p, m_x are the masses of the J/ψ (or ψ'), the proton, and the meson (or γ) in the final state, while A is the total (dimensionless) reaction amplitude. Note that in Eq. (5) we have assumed that averaging over the spin states has been already performed [48]. In the present manuscript we will consider only individual partial wave amplitudes and, therefore, use a specific A_L in Eq. (5).

Let us come back to A^0 and, specifically, to the assumption that it is constant in the region near the $\bar{N}N$ threshold where we perform our calculation. Such an assumption is sensible if there are no dominant one-, two- or even three-particle doorway channels, with masses or thresholds close to the $\bar{N}N$ threshold, for the transition from J/ψ (or ψ') to $\bar{N}N$. For example, a dominant $\bar{N}N$ production via ρ, $\pi\pi$ or $\pi\pi\pi$ intermediate states would definitely not invalidate this assumption. However, a genuine resonance with a mass comparable to the $X(1835)$ found by the BES Collaboration in the reaction $J/\psi \to \gamma\pi^+\pi^-\eta'$ [49,50] would render it already somewhat questionable, if it constitutes indeed the dominant doorway channel for the decay into the $\bar{N}N$ system. In any case, and as in all previous works that exploit FSI effects, it should be clear that the assumption of a constant $\bar{A}_L^0$ is first and foremost a working hypothesis. The question that can be addressed in our study is simply, whether the energy dependence generated by the $\bar{N}N$ interaction in the final state alone suffices to describe the $\bar{p}p$ invariant mass spectra or not. A possible genuine energy dependence of the primary production amplitude itself cannot be excluded.

Conservation of the total angular momentum, together with parity, charge conjugation and isospin conservation for the strong interactions, put strong constraints on the partial waves of the produced $\bar{p}p$ system. We list the allowed quantum numbers for various decay channels in Table I for orbital angular momentum $L \leq 1$, i.e. S and P waves. We use the standard notation $^{(2S+1)}L_J$, where L, S, J are the orbital angular momentum, the total spin and the total angular momentum. The isospin I is sometimes indicated by the notation $^{(2I+1)(2S+1)}L_J$. In the actual calculation we consider, in general, only the lowest partial wave, i.e. either the $^1S_0$ or the $^3S_1$. Those should be the dominant partial waves for energies near the $\bar{p}p$ threshold. As already said, we assume also that a single partial wave saturates (or dominates) in the energy range covered, i.e. up to excess energies of $M(\bar{p}p) - 2m_p \approx 100$ MeV considered also in the earlier works [8,9,13–15,28,29]. In principle, higher partial wave may well play a non-negligible role around 100 MeV (or even at somewhat lower energies)

TABLE I. Allowed $\bar{N}N$ partial waves, J^{PC} assignments and isospins for various channels up to P waves.

Channels	Partial waves	Isospin
$J/\psi \to \gamma\bar{p}p$ $\psi' \to \gamma\bar{p}p$	$^1S_0[0^{-+}], ^3P_0[0^{++}], ^3P_1[1^{++}], ^3P_2[2^{++}]$	0, 1
$J/\psi \to \omega\bar{p}p$ $\psi' \to \omega\bar{p}p$	$^1S_0, ^3P_0, ^3P_1, ^3P_2$	0
$J/\psi \to \rho\bar{p}p$ $\psi' \to \rho\bar{p}p$	$^1S_0, ^3P_0, ^3P_1, ^3P_2$	1
$J/\psi \to \eta\bar{p}p$ $\psi' \to \eta\bar{p}p$	$^3S_1[1^{--}], ^1P_1[1^{+-}]$	0
$J/\psi \to \pi^0\bar{p}p$ $\psi' \to \pi^0\bar{p}p$	$^3S_1, ^1P_1$	1
$\chi_{c0} \to \pi^-\bar{n}p$	$^1S_0, ^3P_1$	1

and one could limit oneself to excess energies up to ≈ 50 MeV, say, to be on the safe side. Or one could introduce a cocktail of amplitudes. However, at present there is very little experimental information to constrain the relative weight of the partial waves and also their interference. Hopefully in the future, with a larger data set and more precise measurements of angular distributions a more refined analysis will become feasible. Note that it is possible that dynamical selection rules lead to a suppression of the lowest partial waves in the $\bar{N}N$ system. This could be also detected by measuring the angular distributions of the decay products.

III. RESULTS

Most of the studies of FSI effects in the reaction $J/\psi \to \gamma \bar{p} p$ (and related decays) in the literature are performed in the Migdal-Watson approach [23,24]. In this approximation, instead of evaluating the integral equation that arises in the DWBA, see Eq. (2), the FSI is simply accounted for by multiplying the elementary reaction amplitude by the on-shell $\bar{N}N$ T-matrix, i.e. $A_L \approx N \cdot \bar{A}_L^0 T_L(k,k;E_k)/k_L$, where N is an arbitrary normalization factor. It is known from pertinent studies that the applicability of the Migdal-Watson approach is limited to a fairly small energy range [46]. In particular, it works only reasonably well if the scattering length is rather large—which is the case for NN scattering with values of $a \approx -24$ fm for the interaction in the (np) $^1S_0$ partial wave. However, for $\bar{N}N$ scattering the values for the scattering lengths are typically in the order of only 1–2 fm [26,30].

Entem and Fernández have presented results based on the Migdal-Watson approximation and on the DWBA [14] and those suggest drastic differences between the two approaches. Indeed, we can confirm this with our own calculation employing the $\bar{N}N$ potential A(OBE) [18] that we used in our earlier studies [8,9,28,29]. Corresponding results are presented in Fig. 1. The dash-dotted curve is the prediction for the $\bar{p}p$ invariant mass based on the $I = 1$ $^1S_0$ amplitude in the Migdal-Watson approximation, as published in Ref. [8] which reproduces rather well the energy dependence found in the experiments [1,51,52]. The result for the same $\bar{N}N$ interaction but based on the more refined treatment of the FSI, Eq. (4), is no longer in agreement with the data, see the solid curve in Fig. 1. At first sight, this is certainly disturbing. However, we want to emphasize that it would be premature to see the observed discrepancy as signal for the failure of the FSI interpretation of the enhancement in the near-threshold $\bar{p}p$ invariant mass spectrum. Rather it could be simply an evidence for certain shortcomings of the employed $\bar{N}N$ interaction in the $^1S_0$ partial wave. In addition, isospin is not conserved in the reaction $J/\psi \to \gamma \bar{p} p$ and, therefore, the actual $\bar{N}N$ FSI can involve any combination of the $I = 0$ and $I = 1$ $^1S_0$ amplitudes. We will address these issues in detail later

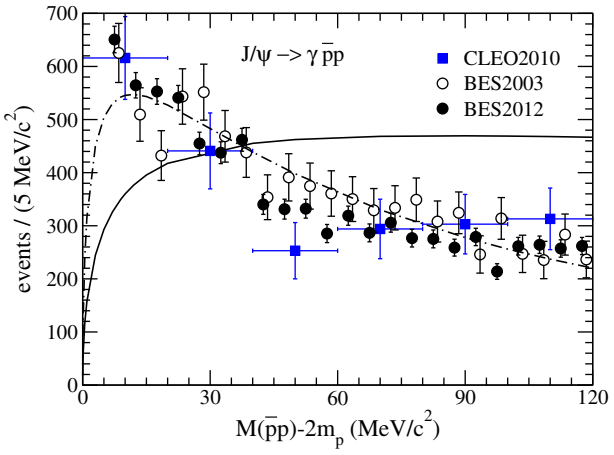

FIG. 1 (color online). $\bar{p}p$ spectrum for the decay $J/\psi \to \gamma \bar{p} p$. The solid curve denotes results for the $\bar{N}N$ interaction A(OBE) based on the DWBA, see Eq. (4), while the dash-dotted curve is based on the Migdal-Watson approximation [8]. Data are taken from Refs. [1,51,52]. The measurement of Ref. [51] is adopted for the scale. The data for the BES measurement from 2003 have been shifted slightly to the right, cf. text.

in this section. First we want to look at purely hadronic (J/ψ and ψ') decay channels with a $\bar{p}p$ final state where nominally isospin is conserved.

But before that we would like to comment on the normalization. Usually only event rates are given for the various experiments. These differ for different experiments and also for different invariant-mass resolutions. For the figures presented below, in general, we fix the scale according to the experiment with the highest resolution. Which data set is used to fix the scale will be emphasized in the pertinent caption. The data (and error bars) from other experiments with lower resolution are then renormalized to this scale, guided by the eye. Also our theory results are renormalized to this scale (guided by the eye) by an appropriate choice of $\bar{A}_L^0$ in Eq. (4). The only exception is the $J/\psi \to \gamma \bar{p} p$ reaction, where the constant $\bar{A}_L^0$ is fixed via a fit to the $\bar{p}p$ invariant-mass spectrum. Note also that the actual values of (most of) the data presented in the various figures were not directly available to us. We use here values obtained from digitizing the figures of the original publications. Finally, for some decays the BES Collaboration has published data sets with different statistics but with the same momentum resolution. Since we wanted to include both sets in the same figure we shifted the ones from the earlier measurement slightly to the right (by 1 MeV) so that one can distinguish the two data sets easier in the figure. This concerns the $\gamma \bar{p} p$ and the $\omega \bar{p} p$ channels.

A. Decays into three hadrons

Besides $J/\psi \to \gamma \bar{p} p$ there is also experimental information on J/ψ and ψ' decays into three-body channels

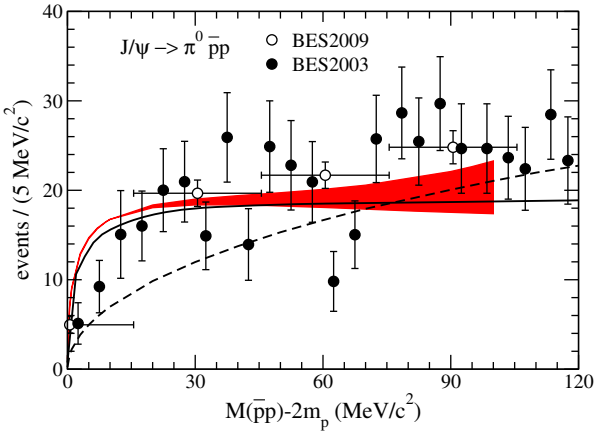

FIG. 2 (color online). $\bar{p}p$ spectrum for the decay $J/\psi \to \pi^0\bar{p}p$. The band represents the result based on the $\bar{N}N$ FSI generated from the chiral EFT potential [30] while the solid curve is the result for the $\bar{N}N$ interaction A(OBE) [18]. The dashed curve denotes the phase space behavior. Data are taken from Refs. [1,53]. The measurement of Ref. [1] is adopted for the scale.

involving a $\bar{p}p$ pair and a pseudoscalar (π, η) [1,52–56] or vector (ω) [57,58] meson. There is, however, a strong variation in the quality of the data. While in case of $J/\psi \to \pi^0\bar{p}p$ and $J/\psi \to \omega\bar{p}p$ the momentum resolution is excellent and comparable to the one for $J/\psi \to \gamma\bar{p}p$, the bin widths for the other reactions are much larger.

Let us first consider channels with pseudoscalar mesons. The processes of J/ψ and ψ' decaying to $\pi\bar{p}p$ or $\eta\bar{p}p$ involve the ${}^3S_1$ partial wave, see Table I. The event rates calculated via Eqs. (4) and (5) are shown in Fig. 2 for the decay $J/\psi \to \pi^0\bar{p}p$, in Fig. 3 for $J/\psi \to \eta\bar{p}p$, in Fig. 4 for $\psi' \to \pi^0\bar{p}p$, and in Fig. 5 for $\psi' \to \eta\bar{p}p$. Results based on our $\bar{N}N$ potential derived in chiral EFT are presented as bands. Chiral EFT interactions for baryon-baryon systems require a regularization when inserted into the LS equation (3) [59–61] and in Ref. [30] this was done in form of an

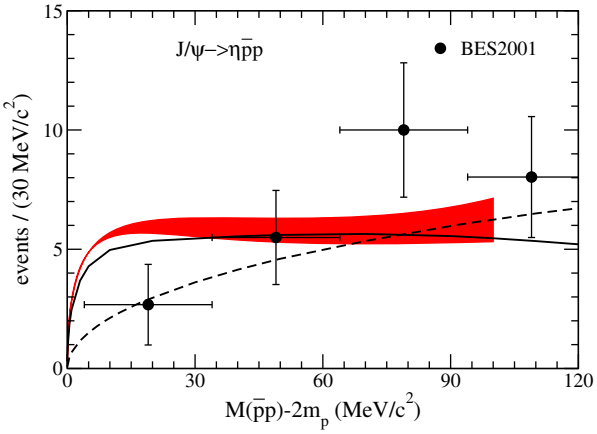

FIG. 3 (color online). $\bar{p}p$ spectrum for the decay $J/\psi \to \eta\bar{p}p$. Same description of curves as in Fig. 2. Data are taken from Ref. [54].

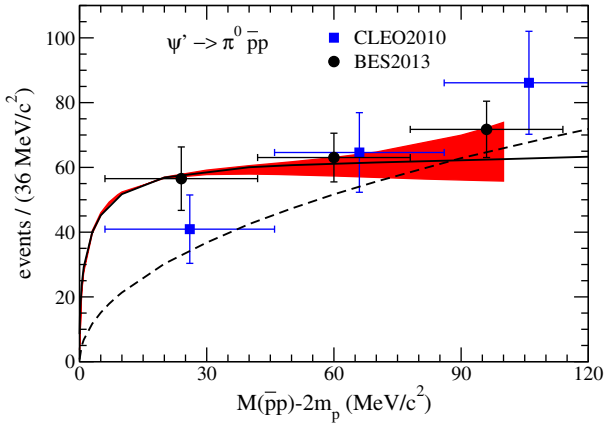

FIG. 4 (color online). $\bar{p}p$ spectrum for the decay $\psi' \to \pi^0\bar{p}p$. Same description of curves as in Fig. 2. Data are taken from Refs. [52,55]. The measurement of Ref. [55] is adopted for the scale.

exponential regulator function that involves a cutoff mass Λ. The cutoff values were chosen in the range $\Lambda = 450$–650 MeV, guided by what was used for chiral nucleon-nucleon potentials in the past [59,60]. Since the two-pion exchange potential is calculated using spectral function regularization [60], there is also a dependence on the pertinent cutoff parameter $\tilde{\Lambda}$, see Ref. [30] for details. The band indicates the variation of our results for the various cutoff combinations $\{\Lambda, \tilde{\Lambda}\}$ considered in the construction of the EFT $\bar{N}N$ potential. It can be viewed as a rough estimate of the theoretical uncertainty (of the $\bar{N}N$ amplitude) as discussed in Ref. [59] (Sec. 3), see also the related discussion in Ref. [61].

The solid line is the prediction for the meson-exchange potential A(OBE). The dashed line represents the phase space behavior and follows from Eq. (5) by setting the production amplitude A to a constant. In general, the latter is normalized in such a way that it coincides with the results

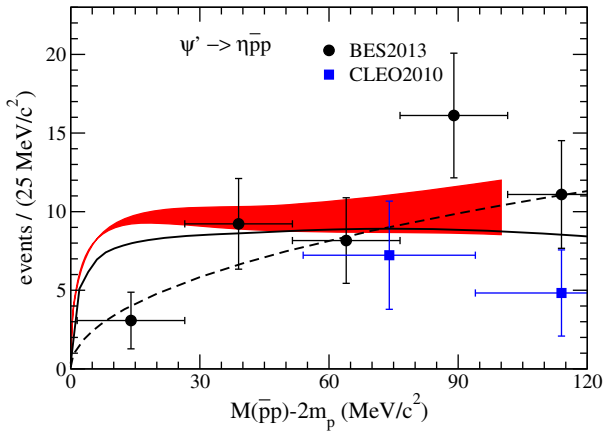

FIG. 5 (color online). $\bar{p}p$ spectrum for the decay $\psi' \to \eta\bar{p}p$. Same description of curves as in Fig. 2. Data are taken from Refs. [52,56]. The measurement of Ref. [56] is adopted for the scale.

for the EFT interaction for excess energies around 70–80 MeV. We want to stress once more that in Fig. 2 and in the other figures in this section all normalizations are arbitrary. We are only interested in the energy dependence as it follows from the FSI effects predicted by the employed $\bar{N}N$ interactions.

Obviously, in all cases our predictions are in line with the data. Specifically, the results for $J/\psi \to \pi^0 \bar{p}p$ are in nice agreement with the experiment. Here the FSI generates a moderate but noticeable enhancement at small $\bar{p}p$ invariant masses as compared to the phase space and yields a $\bar{p}p$ spectrum which is seemingly closer to the trend exhibited by the data than the phase-space curve. It is interesting to see that the results based on the chiral potential and on A(OBE) are fairly similar. In this context let us remind the reader that we had to introduce some phenomenological adjustments in our earlier study based on the Migdal-Watson approximation [and with A(OBE)] in order to be able to reproduce that experimental invariant mass spectrum, cf. Eq. (8) in Ref. [8]. Now the behavior follows directly from the refined treatment of FSI effects via Eq. (4).

The results for the other channels are less conclusive. The invariant-mass resolution in the pertinent measurements is only in the order of 30 MeV or so and, consequently, there are only three or four data points below the excess energy of 100 MeV. Whether or not the present data require the enhancement provided by the $\bar{N}N$ FSI is difficult to judge. Hopefully, future measurements with much higher statistics as well as much higher resolution will provide a more serious test for FSI effects.

Let us now look at the decay $J/\psi \to \omega \bar{p}p$. In this case the $\bar{p}p$ state is produced in the $^1S_0$ partial wave with isospin $I = 0$, cf. Table I. Our results based on the Jülich model A(OBE) [18] (solid curve) and the chiral potential constructed in Ref. [30] (band) are shown in Fig. 6 and compared to data from the BES Collaboration [57,58]. As can be seen from Fig. 6, the predictions agree rather well with the measured $\bar{p}p$ invariant mass spectrum in the energy range considered. Also here differences between the results based on the chiral potential and A(OBE) are small. Actually, it seems that for this particular $\bar{N}N$ partial wave there is no strong dependence on the employed FSI formalism. Our results for A(OBE) based on the Migdal-Watson approximation, published in [28], are qualitatively very similar to the ones we get now within the DWBA.

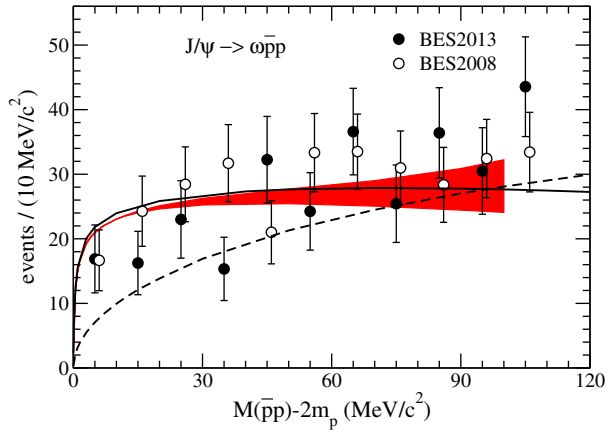

FIG. 6 (color online). $\bar{p}p$ spectrum for the decay $J/\psi \to \omega \bar{p}p$. Same description of curves as in Fig. 2. Data are taken from Refs. [57,58]. The measurement of Ref. [58] is adopted for the scale. The data for the measurement from 2008 have been shifted slightly to the right, cf. text.

B. Radiative decays

In the $J/\psi \to \gamma \bar{p}p$ and $\psi' \to \gamma \bar{p}p$ decays the isospin is no longer conserved and, in principle, the final $\bar{p}p$ state can have any admixture of the isospin 0 and 1 components. In our previous works the $I = 1$ amplitude was used for $J/\psi \to \gamma \bar{p}p$ [8] while for $\psi' \to \gamma \bar{p}p$ the isospin averaged amplitude, $T^{\bar{p}p} = (T^{I=0} + T^{I=1})/2$, was found to yield a good agreement with the measurements [29]. Results based on an $\bar{N}N$ interaction derived from the quark model, presented in Ref. [14], suggest that the FSI effects of both isospin components might be roughly in line with the data, while apparently in Refs. [13,15,17] only the isospin 0 amplitude was considered. The BES Collaboration argues in favor of a decay into a pure $I = 0$ $\bar{p}p$ state, guided by the experimental observation that apparently $I = 1$ states are suppressed in J/ψ radiative decays [49]. Indeed, the branching fraction of $J/\psi \to \gamma\pi^0$ is very small as compared to $J/\psi \to \gamma\eta$ [62]. But one must also say that there are only a few candidates listed in [62] for a decay of J/ψ into γ and a pure $I = 1$ hadronic channel. And, in case of $J/\psi \to \gamma\rho\omega$ for example, only an upper limit of the branching fraction is known.

Note that for the reaction $J/\psi \to \gamma \bar{p}p$ a partial-wave analysis has been performed [51]. It suggests that the near-threshold enhancement is dominantly in the $J^{PC} = 0^{-+}$ state, which means that the $p\bar{p}$ system should be in the $^1S_0$ partial wave.

As already shown above, using the Jülich model A(OBE) as input, the mass dependence of the near-threshold $\bar{p}p$ spectrum (and specifically the pronounced peak) is no longer reproduced when the refined treatment of the FSI is employed. It turns out that the same is also the case for the chiral EFT potential of Ref. [30].

In the present study we adhere to the hypothesis that the enhancement in the $\gamma \bar{p}p$ channel is connected with the $\bar{p}p$ FSI. Then, there are two options: First, we can dismiss the assumption that the produced $\bar{p}p$ state consists only of the $I = 1$ component alone (made in our earlier work [8] and also in the calculation based on the EFT interaction mentioned right above) and allow for an arbitrary mixture of the $I = 0$ and 1 amplitudes. Second, we can question the amplitude in the $^1S_0$ partial wave as predicted by the employed Jülich A(OBE) and chiral EFT $\bar{N}N$ potentials.

Since the one produced by the latter interaction was fixed by a fit to the partial-wave analysis of Zhou and Timmermans [31] this implies that we have to depart from the results of that analysis.

Clearly, for physical (and practical) reasons we still want to stay as close as possible to the solution given in Ref. [31] which reproduces the considered $\bar{N}N$ data very well. Thus, we allow only minimal variations in the $^1S_0$ partial wave and keep all other partial waves fixed. Furthermore, we require that all $\bar{N}N$ scattering observables in the low-energy region remain practically unchanged. This concerns the total, elastic ($\bar{p}p \to \bar{p}p$), and charge-exchange ($\bar{p}p \to \bar{n}n$) cross sections, and also the differential cross sections. Since at low energies those observables are dominated by the $^3S_1$ partial wave and the weight of the $^1S_0$ amplitude is fairly small, there is some freedom for variations even under such strict constraints.

We will consider only variations in the $^{31}S_0$ partial wave, i.e. in the $I = 1$ amplitude. The $^{11}S_0$ potential is kept as in Ref. [30]. Given the fact that the $\bar{p}p$ invariant mass spectrum for $J/\psi \to \omega\bar{p}p$ is well reproduced by the $^{11}S_0$ amplitude we do not see any reasons to introduce modifications in this partial wave. Recall that the $\gamma\bar{p}p$ and $\omega\bar{p}p$ channels involve the very same amplitudes, see the selection rules in Table I. Thus, the assumption that isospin is conserved in the hadronic decay rules out that the strong enhancement seen for $\gamma\bar{p}p$ can be directly associated with FSI effects due to the $I = 0$ amplitude. Indeed, any appreciable modification of the $I = 0$ amplitude would automatically spoil the reproduction of the $\omega\bar{p}p$ data. Note, however, that, in principle, one cannot exclude that isospin conservation is also violated in hadronic decays, see, e.g., Ref. [63].

In the following we examine the two options jointly. We regard two exemplary combinations of the two isospin amplitudes, namely the "standard" one, $T = T^{\bar{p}p} = (T^0 + T^1)/2$, and also one with a predominant $I = 0$ component, $T = (0.7\,T^0 + 0.3\,T^1)$. For both cases we then perform a combined fit to the $\bar{p}p$ invariant mass spectrum for $J/\psi \to \gamma\bar{p}p$ (up to excess energies of 67.5 MeV) and to the $\bar{N}N$ partial-wave cross sections of the $^1S_0$ amplitude as determined in the PWA of Zhou and Timmermans [31]. Results for the $\bar{p}p$ invariant mass spectrum are reported below while details and results for the $\bar{N}N$ sector are summarized in the Appendix.

The decay rate for $J/\psi \to \gamma\bar{p}p$ based on the refitted $\bar{N}N$ interaction is shown in Fig. 7. The results are for the combination $T = (T^0 + T^1)/2$. One can see that now the pronounced peak near 10 MeV is very well described by the FSI. At the same time our (former) $\bar{N}N$ results are also reproduced, cf. the Appendix. Interestingly, the modified potential generates a bound state in the $^{31}S_0$ channel which was not the case for the interaction presented in Ref. [30]. For example, for the cutoff combination

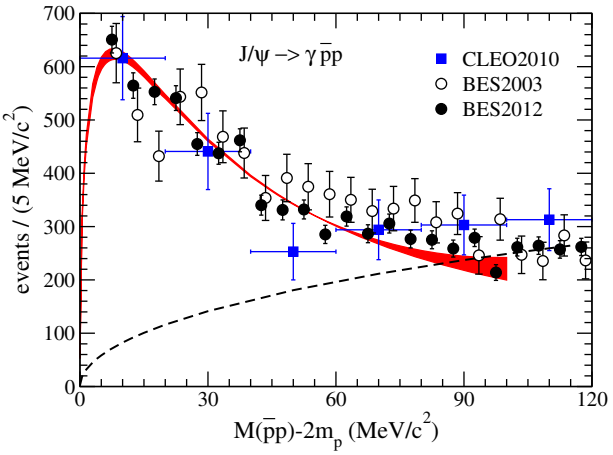

FIG. 7 (color online). $\bar{p}p$ spectrum for the decay $J/\psi \to \gamma\bar{p}p$. The band represents the result with the refitted chiral NNLO potential, see text. The dashed curve denotes the phase space behavior. Data are taken from Refs. [1,51,52]. The measurement of Ref. [51] is adopted for the scale. The data for the BES measurement from 2003 have been shifted slightly to the right, cf. text.

$\{\Lambda, \tilde{\Lambda}\} = \{450\ \text{MeV}, 500\ \text{MeV}\}$ the bound state is located at $E_B = (-36.9 - \text{i}47.20)$ MeV, where the real part denotes the energy with respect to the $\bar{N}N$ threshold. As it happens, this bound state is not very far away from the position of the $X(1835)$ resonance found by the BES Collaboration in the reaction $J/\psi \to \gamma\pi^+\pi^-\eta'$ [49,50]. That resonance was interpreted as a possible signal for a $\bar{N}N$ bound states in several investigations. But, be aware, our bound state is in the $I = 1$ channel *and not* in $I = 0$ as advocated in publications of the BES Collaboration [49] and of other authors [15]. In any case, we want to stress that the actual value we get for the binding energy should be viewed with caution. As mentioned, we examined also the combination $T = 0.7\,T^0 + 0.3\,T^1$, and with it we can achieve likewise a simultaneous description of the $J/\psi \to \gamma\bar{p}p$ data and the $\bar{p}p$ scattering cross section with similar quality. However, in this case the position of the bound state is around $E_B = (-14.8 - \text{i}39.7)$ MeV. Clearly, the data above the $\bar{N}N$ threshold do not allow us to determine the binding energy reliably given that the bound state might be 30 or 40 MeV below the threshold and has a sizable width.

Note that we do not show in Fig. 7 the data points in the lowest bin from the BES experiments. For energies below 5 MeV the Coulomb interaction has a significant influence and likewise the difference between the $\bar{p}p$ and $\bar{n}n$ thresholds plays a role. Both effects are not included in the present calculation. Indeed, because of the strong energy dependence very near threshold, one would need to take into account also the finite momentum resolution of the experiment for a sensible comparison with the data.

There are also experimental results for the decay $\psi' \to \gamma\bar{p}p$ [51,52]. While the statistics is not as high as for the

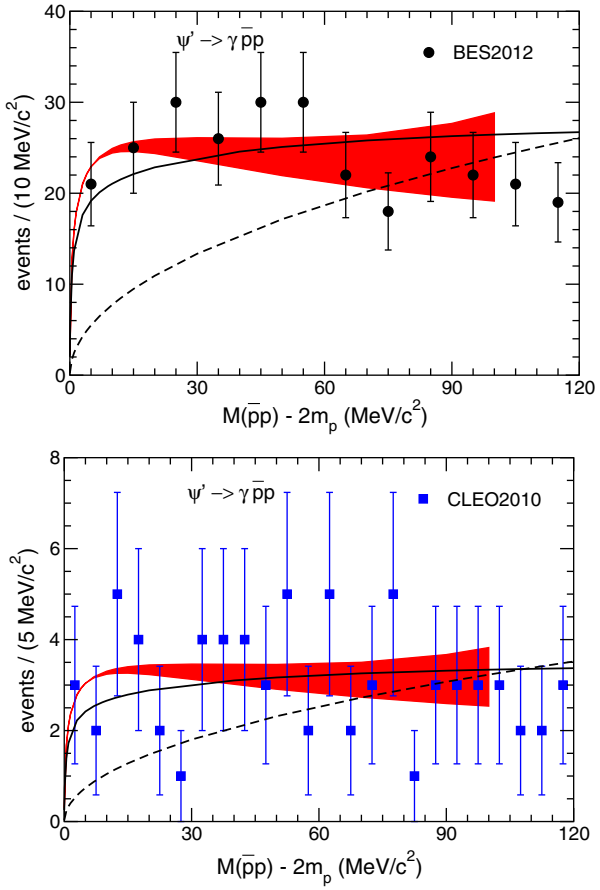

FIG. 8 (color online). $\bar{p}p$ spectrum for the decay $\psi' \to \gamma\bar{p}p$. The band represents the result with the refitted chiral NNLO potential, see text. The solid curve is the result for the $\bar{N}N$ interaction A(OBE) [18]. The dashed curve denotes the phase space behavior. Data are taken from Refs. [51,52].

$J/\psi \to \gamma\bar{p}p$ case, nonetheless, the recent data from the BES Collaboration [51] provide clear evidence that, contrary to $J/\psi \to \gamma\bar{p}p$, in this channel there is no prominent near-threshold peak, but still a significant enhancement as compared to the pure phase-space behavior, see Fig. 8. This is interesting because the quantum numbers of the particles involved in the two reactions are identical and, therefore, one would expect naively to see similar effects from the $\bar{p}p$ FSI. However, in the $\psi' \to \gamma\bar{p}p$ decay isospin is likewise not conserved and, in particular, the reaction amplitude can have a different admixture of the isospin-0 and isospin-1 components. Indeed, when we assume, for example, that for $\psi' \to \gamma\bar{p}p$ the final $\bar{p}p$ state is given by the combination $T = 0.9\,T^0 + 0.1\,T^1$ we can describe the $\bar{p}p$ invariant mass spectrum measured in this reaction very well, as demonstrated in Fig. 8. But a somewhat smaller or larger admixture ($\pm$ 5–10%) of the isospin-0 component would still yield results that are compatible with the data. Note also that the isospin-1 T-matrix from the refitted $^{31}S_0$ potential is employed here, i.e. the same amplitude as in our $J/\psi \to \gamma\bar{p}p$ calculation.

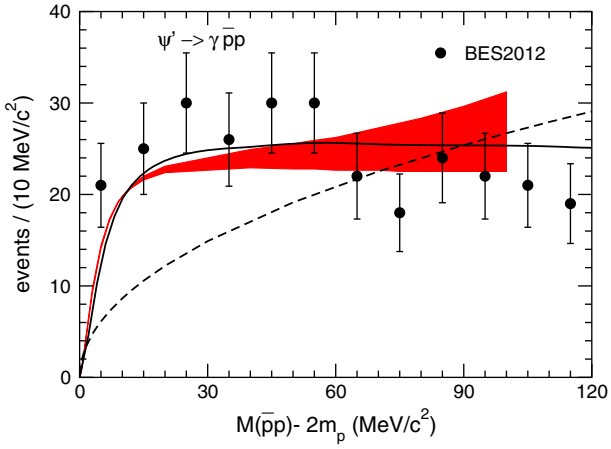

FIG. 9 (color online). $\bar{p}p$ spectrum for the decay $\psi' \to \gamma\bar{p}p$. Same description of curves as in Fig. 8, however, the $^{13}P_0$ partial wave is used for generating the $\bar{N}N$ FSI effects. Data are taken from Ref. [51].

Results based on the $\bar{N}N$ model A(OBE) are also shown in Fig. 8 (solid lines). Here agreement is found for the isospin combination $T = (T^0 + T^1)/2$.

The branching ratios of $\psi' \to \gamma\chi_{cJ}$ ($J = 0,\ 1,\ 2$) are around 10%, for each of the χ_{cJ}'s [62]. Together they amount to about 30%, which is orders of magnitude larger than all other radiative decay modes. Thus, it is quite possible that in the radiative decay of ψ' the $\bar{p}p$ pair is produced predominantly via one of the χ_{cJ} resonances acting as doorway state. If so, then the $\bar{p}p$ state must emerge in a P-wave, see Table I. Therefore, we performed also calculations where we explored such a scenario. It turned out that the assumption of a transition via the χ_{c0} resonance which then leads to a $\bar{p}p$ final state in the $^3P_0$ partial wave yields results that agree fairly well with the data. The corresponding event distribution for the final $\bar{p}p$ pair is presented in Fig. 9 where the isospin-0 amplitude predicted by the considered $\bar{N}N$ interactions was employed. Anyway, the masses of the χ_{cJ}, $J = 0, 1, 2$ states are 3415, 3511, and 3556 MeV, respectively [62]. Thus, the $\bar{N}N$ threshold is very far away from the nominal masses of those resonances and, therefore, only the very tail of the χ_{cJ}'s can contribute to the $\bar{p}p$ spectrum at those low invariant masses considered in our investigation.

C. Discussion

The scenario outlined above allows us to describe consistently (and quantitatively) the near-threshold enhancement seen in the $\bar{p}p$ invariant mass spectrum of various J/ψ and ψ' decays in terms of FSI effects. In particular, we can reproduce the moderate enhancement seen in the reactions $J/\psi \to \omega\bar{p}p$ and $\psi' \to \gamma\bar{p}p$ as well as the rather large enhancement in the $J/\psi \to \gamma\bar{p}p$ channel. The analysis of the latter indicates the possible existence of a $\bar{N}N$ bound state. However, contrary to the suggestion of

the BES Collaboration [49] and the theoretical studies of the Paris group [15], this bound state would be in the isospin-1 channel and not in isospin 0. Therefore, in the following, let us discuss our scenario and possible alternatives in detail.

Near the $\bar{p}p$ threshold the reactions $J/\psi \to \gamma\bar{p}p$, $\psi' \to \gamma\bar{p}p$, and $J/\psi \to \omega\bar{p}p$ are all governed by the same $\bar{N}N$ partial wave, namely the $^1S_0$ (cf. Table I). The assumption that isospin is conserved in the hadronic decay $J/\psi \to \omega\bar{p}p$, together with the observed moderate enhancement in the pertinent $\bar{p}p$ invariant mass spectrum, practically excludes that the exceptionally large enhancement in the $J/\psi \to \gamma\bar{p}p$ decay has anything to do with the isospin-0 $\bar{N}N$ amplitude. Actually, as shown in our analysis, the two measurements can be only reconciled if we assume that the decay into $\gamma\bar{p}p$ involves a substantial isospin-1 amplitude. Of course, it could be possible that there is a strong violation of isospin conservation in the hadronic decay $J/\psi \to \omega\bar{p}p$. However, we believe that this is much less likely than a sizable isospin-1 admixture in the radiative reaction $J/\psi \to \gamma\bar{p}p$ where isospin is not conserved anyway. Another option would be that the decay $J/\psi \to \omega\bar{p}p$ leads predominantly to $\bar{N}N$ P-waves—even close to threshold—and only the reaction $J/\psi \to \gamma\bar{p}p$ is dominated by the decay into the $^1S_0$ partial wave. While a dominance of P-waves might be indeed plausible for $\psi' \to \gamma\bar{p}p$, as discussed above, at the moment there is no experimental evidence that it could be also the case for the ω channel. Clearly, here measurements of the angular distributions for the $\omega\bar{p}p$ case, analogous to those available for $\gamma\bar{p}p$ [51], would be very useful.

What if a genuine resonance is responsible for the enhancement observed in the decay $J/\psi \to \gamma\bar{p}p$? Of course, such a resonance should not couple strongly to the $\bar{N}N$ channel, because otherwise it will contribute significantly to the (direct) $\bar{N}N$ interaction. Then, in turn, it would contribute to the $\bar{N}N$ FSI effects in the pertinent channel, i.e. it should be also seen in $\omega\bar{p}p$, for example. A resonance that couples strongly to J/ψ and only rather weakly to $\bar{N}N$ should be seen in other J/ψ decay channels. In principle, the $X(1835)$ found by the BES Collaboration in the reaction $J/\psi \to \gamma\pi^+\pi^-\eta'$ [49,50] could be a candidate for such a resonance. But then we expect it to be absent in the corresponding reaction $J/\psi \to \omega\pi^+\pi^-\eta'$, say—otherwise one would again have difficulties to explain simultaneously the rather moderate enhancement for the $\omega\bar{p}p$ channel. Indeed, it would be interesting to investigate the latter J/ψ decay channel experimentally.

In any case, the scenario favored by us where the exceptionally strong near-threshold enhancement in the reaction $J/\psi \to \gamma\bar{p}p$ is primarily due to strong FSI effects in the $^1S_0$ $\bar{N}N$ amplitude with isospin $I = 1$ can be tested experimentally. If this scenario is correct then one should see a similarly strong enhancement in other decay channels where near threshold the $\bar{N}N$ system is produced in the same partial wave. This applies first of all to the reaction $J/\psi \to \rho\bar{p}p$ where the $\bar{N}N$ state has to have $I = 1$, provided that isospin is conserved in this strong decay. We present our predictions for the corresponding invariant mass spectrum in Fig. 10.

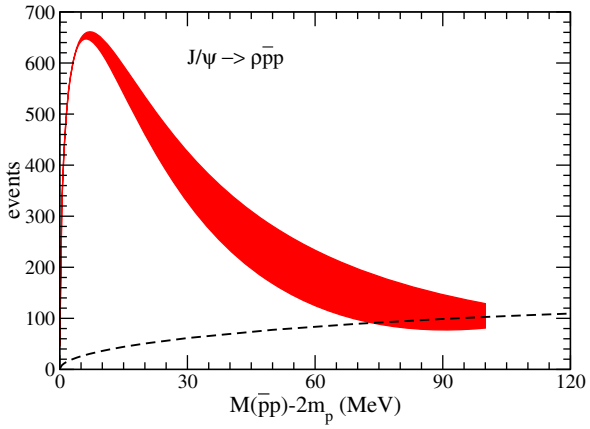

FIG. 10 (color online). $\bar{p}p$ spectrum for the decay $J/\psi \to \rho\bar{p}p$. The band represents the result with the refitted chiral NNLO potential, see text. The dashed curve denotes the phase space behavior.

A measurement of χ_{c0} decaying into $\pi^- p\bar{n}$ would be also rather interesting. In this case, near threshold the $p\bar{n}$ state is likewise produced in the $^1S_0$ partial wave and, moreover, it has to be in isospin $I = 1$, see Table I. Data reported in Ref. [64] suggest that there is a large enhancement in the $p\bar{n}$ invariant mass spectrum in the low-energy region. However, the invariant-mass resolution is still fairly poor and does not allow for any reliable conclusions.

IV. SUMMARY

In the present paper we have provided a systematic analysis of the near-threshold enhancement in the $\bar{p}p$ invariant mass spectrum, as observed in various experiments of the decay reactions $J/\psi \to xp\bar{p}$ and $\psi'(3686) \to xp\bar{p}$, with $x = \gamma, \omega, \pi, \eta$. The enhancement is assumed to be due to the $\bar{N}N$ final-state interaction (FSI) and the pertinent FSI effects are evaluated in an approach that is based on the distorted-wave Born approximation. For the $\bar{N}N$ interaction a potential derived within chiral effective field theory and fitted to results of a recent partial-wave analysis of $\bar{p}p$ scattering data [31] is employed. For comparison, a phenomenological model constructed by the Jülich group and used by us in earlier studies of J/ψ and ψ' decays is also utilized. It is found that the near-threshold spectrum of all considered decay reactions can be reproduced simultaneously and consistently by our treatment of the $\bar{p}p$ FSI. Specifically, the moderate enhancement seen for $\pi^0\bar{p}p$, $\eta\bar{p}p$, and $\omega\bar{p}p$ final states is well described by the $\bar{N}N$ interaction in the relevant $^3S_1$ and $^1S_0$ partial waves as determined in the partial-wave analysis.

The situation is more complicated for the process $J/\psi \to \gamma\bar{p}p$ where there is a rather large near-threshold enhancement. While the pertinent $\bar{p}p$ invariant mass spectrum was reproduced in our previous work [8] that was based on the Migdal-Watson approach, this is no longer the case for the more realistic treatment of FSI effects employed in the present study. However, we can show that a modest modification of the interaction in the $I = 1$ $^1S_0$ $\bar{N}N$ channel—subject to the constraint that the corresponding partial-wave cross sections for $\bar{p}p \to \bar{p}p$ and $\bar{p}p \to \bar{n}n$ remain practically unchanged at low energies—allows one to reproduce the events distribution of the radiative J/ψ decay, and consistently all other decays. In this context the decay $J/\psi \to \omega\bar{p}p$ plays a crucial role. The moderate enhancement observed in this channel, together with the fact that the produced $\bar{p}p$ system has to be in $I = 0$ (assuming that isospin is conserved in this purely hadronic decay) implies that the strong variation seen in the $\gamma\bar{p}p$ case has to come primarily from the $I = 1$ $^1S_0$ $\bar{N}N$ interaction.

It turns out that the modified $I = 1$ $^1S_0$ interaction that can reproduce the $\bar{p}p$ invariant mass spectrum in the reaction $J/\psi \to \gamma\bar{p}p$ predicts a $\bar{N}N$ bound state. Previous investigations suggested that there could be such a bound state, but in the isospin $I = 0$ channel [15]. Also the BES Collaboration favored an $I = 0$ bound state, being led by their observation of the $X(1835)$ resonance in the reaction $J/\psi \to \gamma\pi^+\pi^-\eta'$ [49]. Interestingly, the value we get for the binding energy is comparable to the mass of the $X(1835)$. However, we want to stress that one should view our value with great caution. First, due to the unknown fraction of the $I = 0$ and $I = 1$ components in the final $\bar{p}p$ state for the radiative decay there is a sizable uncertainty in the actual value. Moreover, one should be aware that, in general, any data above the reaction threshold, like the $\bar{p}p$ invariant mass spectrum in the present case, do not allow us to pin down the binding energy reliably given that the bound state might be 30 or 40 MeV below the threshold and has a sizable width. Actually, at this stage we cannot exclude that an alternative fit of similar quality to the invariant mass spectrum and to the near-threshold $\bar{N}N$ scattering data is possible without a bound state in the $I = 1$ $^1S_0$ $\bar{N}N$ partial wave.

Another interesting implication of our study is that $\bar{p}p$ invariant mass spectra as measured in heavy meson decays could be indeed very useful as further constraint for the determination of the $\bar{N}N$ partial-wave amplitudes, provided that those data are of high statistics and high resolution like the ones for $J/\psi \to \gamma\bar{p}p$. This is of specific relevance for the near-threshold region. Here the available $\bar{N}N$ observables are dominated by the $^3S_1$ partial wave whereas the weight of the $^1S_0$ amplitude is fairly small. At such low energies direct $\bar{p}p$ scattering experiments for measuring spin-dependent observables that would allow one to disentangle the spin-singlet and triplet contributions are rather difficult (if not impossible) to perform.

TABLE II. Low-energy constants up to NNLO for the different cutoff combinations $\{\Lambda(\mathrm{MeV}), \tilde{\Lambda}(\mathrm{MeV})\}$. The values of the $\tilde{C}_i$ are in units of 10^4 GeV^{-2} and the C_i in 10^4 GeV^{-4}. The parameters related to annihilation, $\tilde{C}_i^a$ and C_i^a [see Eq. (A1)] are in units of 10^2 GeV^{-1} and 10^2 GeV^{-3}, respectively.

LEC		$\{450, 500\}$	$\{650, 500\}$	$\{450, 700\}$	$\{650, 700\}$
$I = 1$	$\tilde{C}_{^1S_0}$	0.111	0.035	0.096	0.005
	$C_{^1S_0}$	0.080	1.273	0.729	2.022
	$\tilde{C}^a_{^1S_0}$	−0.263	−0.204	−0.288	−0.333
	$C^a_{^1S_0}$	4.876	1.541	4.732	1.935

ACKNOWLEDGMENTS

One of the authors (XWK) acknowledges communications with Prof. Changzheng Yuan concerning the status of the various BES experiments. This work is supported in part by the DFG and the NSFC through funds provided to the Sino-German CRC 110 "Symmetries and the Emergence of Structure in QCD" and by the EU Integrated Infrastructure Initiative HadronPhysics3.

APPENDIX: $\bar{N}N$ INTERACTION IN THE $^1S_0$ PARTIAL WAVE

A comprehensive description of our $\bar{N}N$ potential derived within chiral EFT can be found in Ref. [30], where all technical details are given. Here we focus only on those ingredients that are relevant for the alternative description of the $^1S_0$ partial wave with isospin $I = 1$ that is employed in Sec. III. In this case a refit of the low-energy constants (LECs) in the contact terms was performed. Up to next-to-next-to-leading order (NNLO) the corresponding contribution to the potential is given by [30]

TABLE III. $^1S_0$ scattering lengths a and hadronic shifts and broadenings in hyperfine states of $\bar{p}$H for 1^1S_0. Results based on the refitted $^{31}S_0$ LECs are given and compared with the ones given in Ref. [30] and with empirical information. The $^{11}S_0$ scattering length is taken over from Ref. [30].

	Present work	Reference [30]	Experiment
$a^{I=0}$ (fm)	$-0.21 - \mathrm{i}(1.21 \cdots 1.22)$		
$a^{I=1}$ (fm)	$(0.97 \cdots 1.07) - \mathrm{i}(0.63 \cdots 0.70)$	$(1.02 \cdots 1.04) - \mathrm{i}(0.57 \cdots 0.61)$	
ΔE (eV)	$-(329 \cdots 376)$	$-(302 \cdots 361)$	-740 ± 150 [65] -440 ± 75 [66]
Γ (eV)	$(1596 \cdots 1659)$	$(1545 \cdots 1589)$	1600 ± 400 [65] 1200 ± 250 [66]

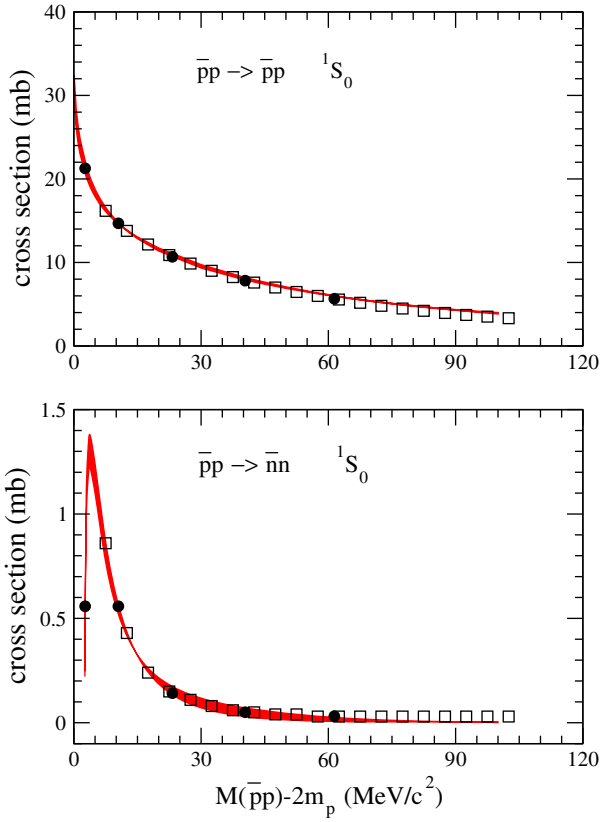

FIG. 11 (color online). The $^1S_0$ partial-wave cross sections as a function of the excess energy. The squares represent the results for the published NNLO potential [30] with the cutoff combination $\{450\ \text{MeV}, 500\ \text{MeV}\}$. The circles indicate the cross sections for the partial-wave amplitudes of Ref. [31]. The bands show the results based on the refitted isospin-1 $^1S_0$ amplitudes.

$$\begin{aligned}\mathrm{Re}V(^1S_0) &= \tilde{C}_{^1S_0} + C_{^1S_0}(p^2 + p'^2)\\ \mathrm{Im}V(^1S_0) &= V_{\mathrm{ann}}(^1S_0)\\ &= -i(\tilde{C}^a_{^1S_0} + C^a_{^1S_0}p^2)(\tilde{C}^a_{^1S_0} + C^a_{^1S_0}p'^2), \qquad \text{(A1)}\end{aligned}$$

where $p(p')$ is the modulus of the three-momentum for the initial (final) state in the center-of-mass system (CMS). In Ref. [30], the values for these LECs $\tilde{C}_{^1S_0}, \ldots, C^a_{^1S_0}$ were obtained by fitting to the results of the partial-wave analysis (PWA) for this particular partial wave provided in Ref. [31].

Now the LECs appearing in the $^{31}S_0$ potential in Eq. (A1) are fitted to both, the $\bar{N}N$ $^{31}S_0$ partial-wave cross section up to laboratory energies of 125 MeV and the $J/\psi \to \gamma\bar{p}p$ event distribution (up to excess energies of 67.5 MeV). With regard to the partial-wave cross section we fit to the one produced by the original NNLO interaction of Ref. [30]. This makes sure that we stay also as close as possible to the results of the PWA from Ref. [31]. As can be seen in Ref. [30] the phase shifts and inelasticities of our EFT potential are basically identical to the ones from the PWA up to laboratory energies of around 125 MeV. The LECs resulting from the fitting procedure are listed in Table II. In this context we want to mention that there is a mistake in Tables 1 and 2 of Ref. [30], i.e. in the list of the LECs for our original NLO and NNLO interactions. In case of the $^1S_0$ partial wave the parameters for $C_{^1S_0}$ and $\tilde{C}^a_{^1S_0}$ are mixed up (for both isospins). For example, this means that the parameters given in the 2nd line are those for $\tilde{C}^a_{^1S_0}$ and the ones in the 3rd line are those for $C_{^1S_0}$.

Let us first look at the scattering length and compare the present one with that of the original interaction [30],

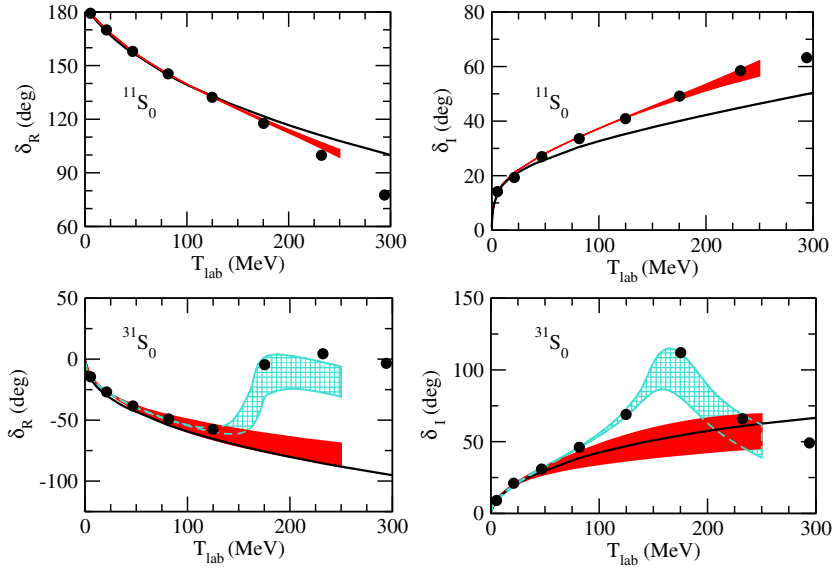

FIG. 12 (color online). Real and imaginary parts of the phase shift in the $^1S_0$ partial waves. The filled bands show results for the employed EFT interaction up to NNLO. The isospin-1 phase shifts for the original NNLO potential [30] are indicated by the hatched band. The solid line is the result for A(OBE). The circles represent the solution of the partial-wave analysis of Ref. [31].

cf. Table III. The corresponding level shifts and widths for the antiproton hydrogen in the state of 1^1S_0 are also compiled in that table. From these numbers we see that the predictions with the modified $^{31}S_0$ potential agree with the original ones within the uncertainty induced by the cutoff variation. We provide here also some experimental information on these quantities [65,66], though we want to stress that additional assumptions have to be made in order to deduce the splitting of the 1^1S_0 level shift from the experiment [26,67].

The resulting $^1S_0$ partial cross sections for the reactions $\bar{p}p \to \bar{p}p$ and $\bar{p}p \to \bar{n}n$ are displayed in Fig. 11. Here the squares represent the results for the published NNLO potential [30] with the cutoff $\{450\ \mathrm{MeV}, 500\ \mathrm{MeV}\}$ while the bands show our calculation with the refitted isospin-1 $^1S_0$ amplitude. We see that the latter reproduces the former results very well. The circles are the partial-wave cross sections for the PWA of Ref. [31].

Finally, in Fig. 12 we present phase shifts for the $^1S_0$ partial wave. Here the results from the refit are shown by a filled band while those of the published NNLO potential [30] are indicated by the hatched band. For convenience we reproduce here also the results for the isospin 0 case from [30] and those of the employed Jülich $\bar{N}N$ potential.

[1] J. Z. Bai *et al.* (BES Collaboration), Phys. Rev. Lett. **91**, 022001 (2003).
[2] A. Datta and P. J. O'Donnell, Phys. Lett. B **567**, 273 (2003).
[3] G. J. Ding and M. L. Yan, Phys. Rev. C **72**, 015208 (2005).
[4] M. L. Yan, S. Li, B. Wu, and B.-Q. Ma, Phys. Rev. D **72**, 034027 (2005).
[5] N. Kochelev and D. P. Min, Phys. Lett. B **633**, 283 (2006).
[6] B. A. Li, Phys. Rev. D **74**, 034019 (2006).
[7] X. G. He, X. Q. Li, X. Liu, and J. P. Ma, Eur. Phys. J. C **49**, 731 (2007).
[8] A. Sibirtsev, J. Haidenbauer, S. Krewald, U.-G. Meißner, and A. W. Thomas, Phys. Rev. D **71**, 054010 (2005).
[9] J. Haidenbauer, U.-G. Meißner, and A. Sibirtsev, Phys. Rev. D **74**, 017501 (2006)
[10] B. Kerbikov, A. Stavinsky, and V. Fedotov, Phys. Rev. C **69**, 055205 (2004).
[11] D. V. Bugg, Phys. Lett. B **598**, 8 (2004).
[12] B. S. Zou and H. C. Chiang, Phys. Rev. D **69**, 034004 (2004).
[13] B. Loiseau and S. Wycech, Phys. Rev. C **72**, 011001 (2005).
[14] D. R. Entem and F. Fernández, Phys. Rev. D **75**, 014004 (2007).
[15] J.-P. Dedonder, B. Loiseau, B. El-Bennich, and S. Wycech, Phys. Rev. C **80**, 045207 (2009).
[16] G.-Y. Chen, H. R. Dong, and J. P. Ma, Phys. Lett. B **692**, 136 (2010).
[17] S. Wycech, J. P. Dedonder, and B. Loiseau, EPJ Web Conf. **81**, 05029 (2014).
[18] T. Hippchen, J. Haidenbauer, K. Holinde, and V. Mull, Phys. Rev. C **44**, 1323 (1991).
[19] V. Mull, J. Haidenbauer, T. Hippchen, and K. Holinde, Phys. Rev. C **44**, 1337 (1991).
[20] V. Mull and K. Holinde, Phys. Rev. C **51**, 2360 (1995).
[21] B. El-Bennich, M. Lacombe, B. Loiseau, and S. Wycech, Phys. Rev. C **79**, 054001 (2009).
[22] D. R. Entem and F. Fernández, Phys. Rev. C **73**, 045214 (2006).
[23] K. M. Watson, Phys. Rev. **88**, 1163 (1952).
[24] A. B. Migdal, JETP **1**, 2 (1955).
[25] C. Hanhart, Phys. Rep. **397**, 155 (2004).
[26] D. Gotta, Prog. Part. Nucl. Phys. **52**, 133 (2004).
[27] M. L. Goldberger and K. M. Watson, *Collision Theory* (John Wiley and Sons, New York, 1964), Chap. 9.3.
[28] J. Haidenbauer, U.-G. Meißner, and A. Sibirtsev, Phys. Lett. B **666**, 352 (2008).
[29] J. Haidenbauer and U.-G. Meißner, Phys. Rev. D **86**, 077503 (2012)
[30] X.-W. Kang, J. Haidenbauer, and U.-G. Meißner, J. High Energy Phys. 02 (2014) 113.
[31] D. Zhou and R. G. E. Timmermans, Phys. Rev. C **86**, 044003 (2012).
[32] K. Abe *et al.* (Belle Collaboration), Phys. Rev. Lett. **88**, 181803 (2002).
[33] K. Abe *et al.* (Belle Collaboration), Phys. Rev. Lett. **89**, 151802 (2002).
[34] J. T. Wei *et al.* (Belle Collaboration), Phys. Lett. B **659**, 80 (2008).
[35] B. Aubert *et al.* (*BABAR* Collaboration), Phys. Rev. D **74**, 051101 (2006).
[36] P. del Amo Sanchez *et al.* (*BABAR* Collaboration), Phys. Rev. D **85**, 092017 (2012)
[37] R. Aaij *et al.* (LHCb Collaboration), Phys. Rev. D **88**, 052015 (2013).
[38] R. Aaij *et al.* (LHCb Collaboration), Phys. Rev. Lett. **113**, 141801 (2014).
[39] S. B. Athar *et al.* (CLEO Collaboration), Phys. Rev. D **73**, 032001 (2006).
[40] J. Haidenbauer, H. W. Hammer, U.-G. Meißner, and A. Sibirtsev, Phys. Lett. B **643**, 29 (2006).
[41] J. Haidenbauer, X.-W. Kang, and U.-G. Meißner, Nucl. Phys. **A929**, 102 (2014).
[42] G. Bardin *et al.*, Nucl. Phys. **B411**, 3 (1994).
[43] A. Antonelli *et al.*, Nucl. Phys. **B517**, 3 (1998).
[44] J. P. Lees *et al.*, Phys. Rev. D **87**, 092005 (2013).
[45] C. Hanhart and K. Nakayama, Phys. Lett. B **454**, 176 (1999).
[46] V. Baru, A. M. Gasparian, J. Haidenbauer, A. E. Kudryavtsev, and J. Speth, Yad. Fiz. **64**, 633 (2001) [Phys. At. Nucl. **64**, 579 (2001)].

[47] A. Gasparyan, J. Haidenbauer, and C. Hanhart, Phys. Rev. C **72**, 034006 (2005).
[48] E. Byckling and K. Kajantie, *Partical Kinematics* (John Wiley and Sons, New York, 1973).
[49] M. Ablikim *et al.* (BES Collaboration), Phys. Rev. Lett. **95**, 262001 (2005).
[50] M. Ablikim *et al.* (BESIII Collaboration), Phys. Rev. Lett. **106**, 072002 (2011).
[51] M. Ablikim *et al.* (BESIII Collaboration), Phys. Rev. Lett. **108**, 112003 (2012).
[52] J. P. Alexander *et al.* (CLEO Collaboration), Phys. Rev. D **82**, 092002 (2010).
[53] M. Ablikim *et al.* (BES Collaboration), Phys. Rev. D **80**, 052004 (2009).
[54] J. Z. Bai *et al.* (BES Collaboration), Phys. Lett. B **510**, 75 (2001).
[55] M. Ablikim *et al.* (BESIII Collaboration), Phys. Rev. Lett. **110**, 022001 (2013).
[56] M. Ablikim *et al.* (BESIII Collaboration), Phys. Rev. D **88**, 032010 (2013).
[57] M. Ablikim *et al.* (BES Collaboration), Eur. Phys. J. C **53**, 15 (2008).
[58] M. Ablikim *et al.* (BESIII Collaboration), Phys. Rev. D **87**, 112004 (2013).
[59] E. Epelbaum, W. Glöckle, and U.-G. Meißner, Eur. Phys. J. A **19**, 125 (2004).
[60] E. Epelbaum, W. Glöckle, and U.-G. Meißner, Nucl. Phys. **A747**, 362 (2005).
[61] E. Epelbaum, H. Krebs, and U.-G. Meißner, arXiv: 1412.0142.
[62] K. A. Olive *et al.* (Particle Data Group), Chin. Phys. C **38**, 090001 (2014).
[63] M. Ablikim *et al.* (BESIII Collaboration), Phys. Rev. D **86**, 032008 (2012).
[64] M. Ablikim *et al.* (BESIII Collaboration), Phys. Rev. D **86**, 052011 (2012)
[65] M. Ziegler *et al.* (ASTERIX Collaboration), Phys. Lett. B **206**, 151 (1988).
[66] M. Augsburger *et al.*, Nucl. Phys. **A658**, 149 (1999).
[67] D. Gotta (private communication).